

Structure-Based Design of FXIIIa-Blockers: Addressing a Transient Hydrophobic Pocket in the Active Site of FXIIIa

Martin Stieler,^[a] Christian Büchold,^[b] Marisa Schmitt,^[b] Andreas Heine,^[a] Martin Hils,^[b] Ralf Pasternack,^[b] and Gerhard Klebe^{*[a]}

Blood coagulation factor XIII (FXIII, F13) is considered to be a promising target for anticoagulants with reduced bleeding risk because of its unique position in the coagulation cascade downstream of thrombin. However, until now, no potent drug addressing FXIII has been available, indeed no compound has even entered clinical trials yet. In 2013, we published the co-crystal structure of FXIII in the active state (FXIIIa^o), thereby providing a detailed map of the active site for the rational design of potent FXIIIa blockers. Here we report, for the first time, a structure-based approach to improving the affinity of

FXIIIa inhibitors. FXIII was crystallized in complex with a methyl thiazole moiety to address a novel transient hydrophobic pocket close to the catalytic center. By subsequent structure-based design to rationalize the introduction of an ethyl ester, the potency of the inhibitor was improved significantly compared to that of the parent lead compound. The occupancy of the hydrophobic pocket described here might turn out to be a key step in the development of a potent reversible and orally available FXIIIa blocker.

Introduction

Blood coagulation factor XIII belongs to the transglutaminase enzyme class catalyzing the covalent linkage of proteins or peptides by transamidation between the γ -carboxamide group of glutamine and the ϵ -amino group of lysine, also designated as protein crosslinking.^[1]

The human transglutaminase family comprises eight catalytically active enzymes (TG1–TG7 and FXIII). The prevalent physiological function of TGs is to improve the stability of protein structures in a tightly controlled manner by said crosslinking.^[1] For example, TG2 (tissue transglutaminase) plays a major role in the assembly and remodeling of the extracellular matrix.^[2] TG1, TG3 and TG5 are involved in the formation of the cornified cell envelope^[3–5] and FXIII stabilizes blood clots.^[6] Moreover, with their ability to modify proteins post-translationally, TGs exhibit a regulative function as well,^[1,7] whereas TG2 can even act as a G-protein^[8] and kinase.^[9–10]

Due to a progressive knowledge concerning physiological functions of transglutaminases and their involvement in a variety of disease processes, this enzyme class has increasingly evolved pharmacological interest in the last decades.^[11] Blood


coagulation factor XIII represents a promising target in thrombotic diseases^[12–14] and ZED3197 has been published as the first drug-like and highly potent inhibitor.^[15] TG2 is considered being a promising target for treatment of celiac disease^[7,14,16] and fibrotic disorders such as diabetic nephropathy.^[17] Additionally, tissue transglutaminase is involved in the regulation of cell growth and apoptosis.^[18] Thus, TG2 gains increasingly attention within the scope of cancer therapy.^[19]


Thromboembolic events such as stroke, pulmonary embolism and acute coronary syndrome are among the leading causes of mortality and morbidity. The administration of anticoagulants reduces the occurrence of a thrombus in risk patients but unfortunately enhance the bleeding tendency. This is attributed to the direct or indirect interference of all current anticoagulants with thrombin representing the central enzyme of the blood coagulation cascade (Figure 1). Thrombin activates platelets and fibrinogen resulting in a “soft” clot. Factor XIII, also activated by thrombin, finally stabilizes the clot by forming isopeptide bonds between the fibrin fibers.^[1,20–21] Accordingly, FXIII is the only enzyme in the coagulation cascade acting downstream of thrombin. Consequently, inhibition of FXIII would still allow the formation of a “soft” blood clot. These features render FXIII as a promising target for the development of anticoagulants with a potentially lower bleeding risk compared to current anticoagulants. In addition to its involvement in blood coagulation, FXIII also decorates the clot with α_2 -antiplasmin, lowering fibrinolysis of the mature clot by plasmin.^[22] As a result, inhibition of FXIII would accelerate clot degradation by patient’s own fibrinolytic systems.

A promising strategy to obtain compounds for treatment of a disease, e.g. thrombosis, follows the approach of structure-based drug design. But this requires a crystal structure of the target protein providing detailed information of the active site at atomic level. The crystal structure of factor XIII in the inactive

[a] Dr. M. Stieler, Prof. Dr. A. Heine, Prof. Dr. G. Klebe
Department of Pharmaceutical Chemistry
Philipps-Universität
Marbacher Weg 6, 35032 Marburg (Germany)
E-mail: klebe@staff.uni-marburg.de

[b] Dr. C. Büchold, M. Schmitt, Dr. M. Hils, Dr. R. Pasternack
Zedira GmbH
Roesslerstrasse 83, 64293 Darmstadt (Germany)

 Supporting information for this article is available on the WWW under <https://doi.org/10.1002/cmdc.202000056>

 © 2020 The Authors. Published by Wiley-VCH Verlag GmbH & Co. KGaA. This is an open access article under the terms of the Creative Commons Attribution Non-Commercial License, which permits use, distribution and reproduction in any medium, provided the original work is properly cited and is not used for commercial purposes.

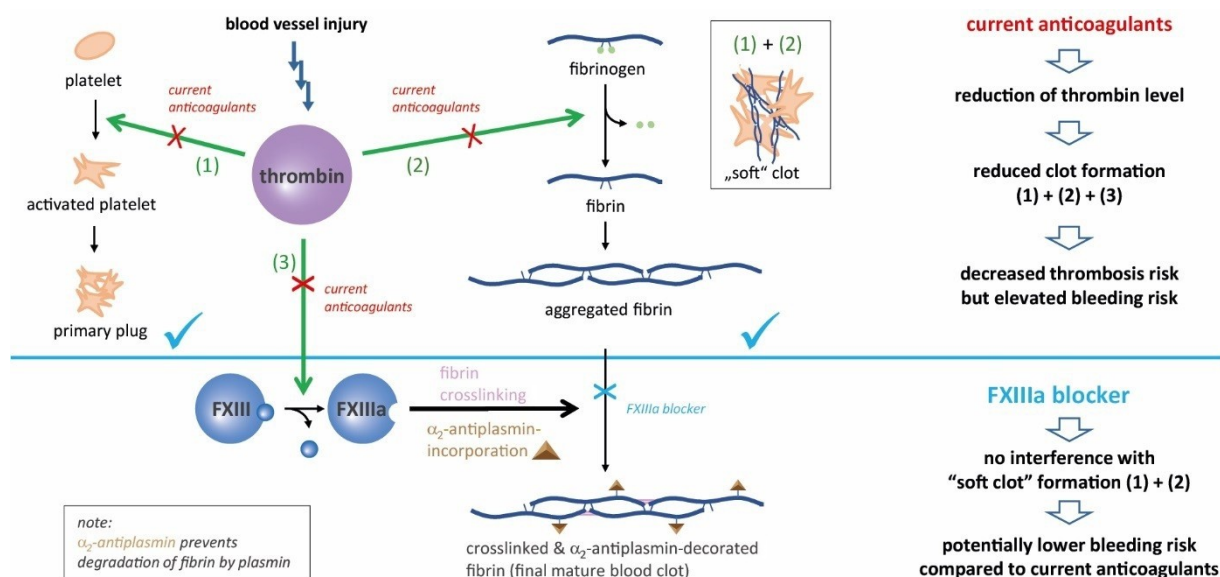


Figure 1. Mode of action of direct-acting FXIIIa blockers compared to current anticoagulants illustrated by a simplified cartoon of the blood coagulation cascade. FXIII is the last enzyme in the coagulation cascade catalyzing fibrin crosslinking and α_2 -antiplasmin incorporation. All current anticoagulants reduce the level of active thrombin. As a result, platelet activation (1), the cleavage of fibrinopeptides (2) and the activation of FXIII (3) are blocked (red cross). In contrast, the inhibition of FXIII still allows primary plug formation (1) and fibrinogen activation (2) without stabilizing the formed clot by crosslinking (3). Thus, administration of a FXIIIa blocker has a significantly reduced impact on hemostasis than do current anticoagulants. Consequently, FXIII can be considered a promising target for novel compounds with an expected lower bleeding risk.

state, published in 1994, was an important milestone of academic research for the transglutaminase community. However, the structure is hardly useful for structure-based design of a FXIII blocker because the active site is buried by the β -barrel 1 domain and the binding mode of substrates and inhibitors remained unclear.^[23]

In 2013, we published a high-resolution crystal structure of blood coagulation factor XIII in the active conformation by co-crystallization of FXIII with the covalent mechanism-based inhibitor ZED1301 (Figure 2A and 3).^[24] Herein, the β -barrel 1 domain of the target does not cover the active site any longer but is located laterally of the catalytic domain.

ZED1301 (**1**) is of octapeptide size composed of an N-terminal acetylated D-aspartate occupying the α -space, followed by the warhead that replaces the former substrate glutamine residue, and forms a covalent bond with the active-site cysteine (C314). Next, three hydrophobic amino acids (two norleucines and a leucine) together with a proline bridge the distance to the hydrophobic pocket in the β -space which accommodates the indole ring of a tryptophan. Another proline residue completes the C-terminus of the peptidic lead structure.

Comparing the α -space of the active (Figure 2B) and inactive state (Figure 2C) of FXIII reveals that a salt bridge formed between the side chain of Arg223 and the N-terminal D-aspartate of **1** seals a transient hydrophobic pocket in the α -space. However, according to its length, this salt bridge can be classified as rather weak (3.6 Å). Therefore, this geometry likely competes with an alternative rotameric conformation of Arg223 where hydrogen bonds can be formed to the backbone carbonyl oxygen of Ser224 and Trp292 (not shown). Consequently, the side chain of Arg223 can exist in two conforma-

tions likely with a similar occupancy as detailed in Figure 2B. As a result, a small transient pocket of hydrophobic nature is opened in the α -space (Figure 2C).

In general, the reversible inhibition of enzymes possessing an active site located on the surface is a challenging mission. Regularly, only the occupancy of hydrophobic pockets provides the required affinity to obtain highly potent inhibitors. Additional to the difficulty concerning the surface exposure of the active site, FXIII undergoes an excessive conformational change from the inactive to the active state.^[24] Most likely, the active state is only adapted in the presence of calcium ions and a substrate or an inhibitor. Thus, the inhibitor needs to be more potent than inhibitors that bind to a conventional target that already adopts its active conformation without a ligand. Hence, addressing the hydrophobic pocket in the α -space may be a key element to develop reversible and low-molecular-weight FXIIIa blockers.

Results and Discussion

During the lead optimization campaign, two novel inhibitors (**2** and **3**) were synthesized bearing moieties to address the hydrophobic pocket in the α -space and replacing the Ac-D-Asp terminus (Figure 3). Inhibitor **2** (ZED1630) possesses a methylated thiazole heterocycle at the N-terminus. Additionally, the compound differs from **1** in that the second norleucine is replaced by an isoleucine and the terminal proline was dispensed. The modified lead binds to FXIIIa with 139 nM potency (Table 1).

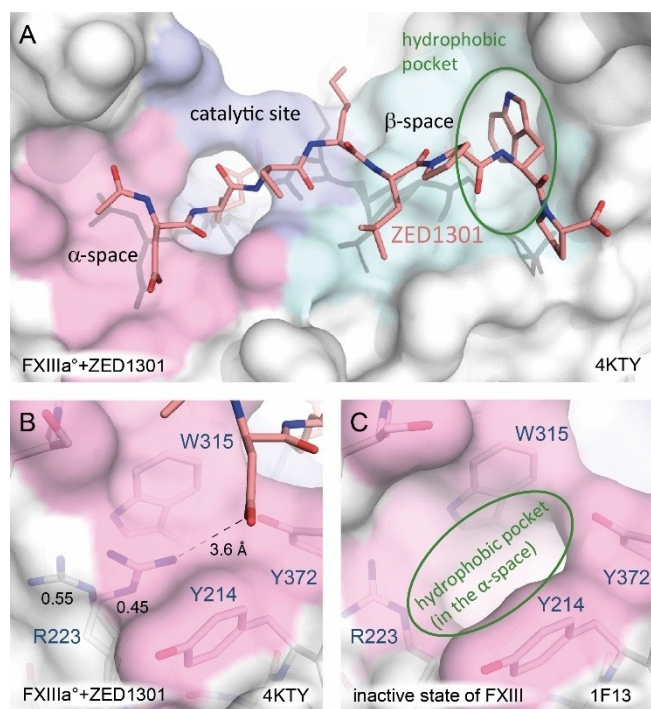


Figure 2. A) The inhibitor ZED1301 (**1**, light red) is covalently attached to Cys314 (not shown) of the catalytic site colored in purple (PDB ID: 4KTY). The acetylated (Ac protecting group) aspartate binds to the α -space (pink), and the indole ring occupies a hydrophobic pocket in the β -space (light blue) guided by the neighboring proline. B) In the α -space, ZED1301 interacts via its aspartate side chain carboxylate oxygen with the guanidinium head group of Arg223 resulting in the closed conformation of the transient pocket. The latter residue is present in the crystal structure in two alternative conformations. They differ by the orientation of the polar head group, which swings around and opens the transient pocket. The ratio of the two conformational states of Arg223 was refined to be 0.55:0.45, as indicated. C) In the inactive state of the enzyme (PDB ID: 1F13), Arg223 adopts only one conformation (β -barrel 1 domain was truncated to uncover the active site). Consequently, the hydrophobic pocket under consideration is completely open.

Regarding the crystal structure of FXIIIa^o in complex with **2**, the thiazole occupies the α -space in a novel manner (Figure 4). The methyl group is perfectly positioned above the targeted hydrophobic pocket. Furthermore, the inhibitor binds significantly closer to the protein surface compared to **1** (difference of the distances between C $_{\alpha}$ of the N-terminal aspartate and the corresponding atom of **2** and the phenolic oxygen Tyr372 amounts 1.3 Å), suggesting an improved binding geometry.

Finally, the indole ring of **2** binds deeper into the hydrophobic pocket (1 Å), and the indole nitrogen forms a buried hydrogen bond to the carbonyl oxygen of Asp367 with a distance of 2.9 Å. It should be mentioned that Asp367 is one of the residues coordinating a calcium ion at binding site 2, and Asp367 adopts this geometry only after the calcium ion is bound to the enzyme as part of the activation process.^[24] Also the proline adjacent to the terminal tryptophan adopts a different spatial orientation in the binding modes of both inhibitors (C $_{\alpha}$ -distance: 1.4 Å). These spatial deviations of **2** and **1** might be caused by the lack of a terminal proline in **2**.

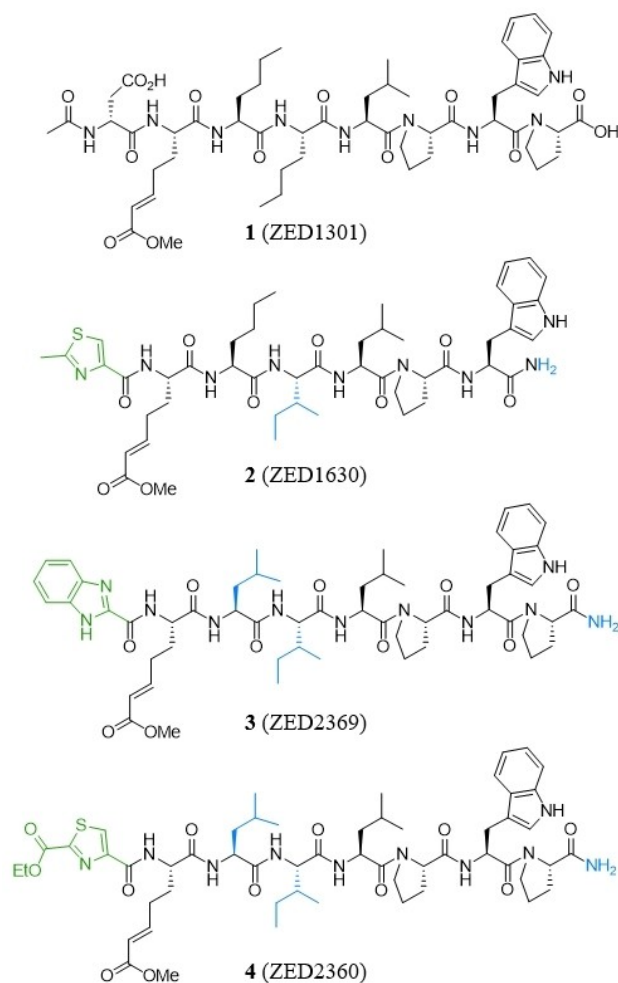


Figure 3. Set of FXIII inhibitors with similar structures. The differences from the lead compound **1** are marked in blue; the N-terminal heterocycles pointing to the α -space are labeled in green. All compounds share the Pro-Trp dipeptide unit, which is essential to occupy the hydrophobic pocket within the β -space as detailed in Figure 2A.

Table 1. Inhibitors with their modifications in the α -space and affinity as well as resolution and PDB ID of the corresponding crystal structure.

Inhibitor	α -Space moiety	IC ₅₀ [nM] ^[a]	Res. [Å]	PDB ID
1 (ZED1301)		110	1.98	4KTY
2 (ZED1630)		139	2.12	5MHM
3 (ZED2369)		102	2.92	5MHO
4 (ZED2360)		29	2.48	5MHN

[a] Determined by FXIIIa isopeptidase assay (see the Experimental Section).

The subsequent compound **3** (ZED2369) possesses a bulky and hydrophobic benzimidazole moiety, along the backbone

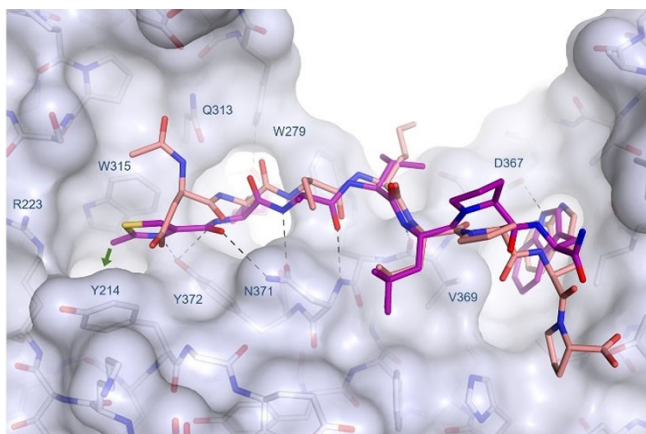


Figure 4. Interaction pattern of **2** (magenta, PDB ID: 5MHM) with FXIIIa^o compared to **1** (light red, PDB ID: 4KTY). The methyl group of the thiazole ring is perfectly positioned in the α -space to address the hydrophobic pocket (green arrow). The indole ring of the C-terminal tryptophan penetrates deeper into the other hydrophobic pocket. The adjacent prolines adopt a different spatial orientation, leading to a C_{α} distance of 1.4 Å. These changes are probably explained by the lack of terminal proline in the truncated compound.

the two norleucines are replaced by leucine and isoleucine, respectively. The C-terminus is identically amidated as in **2**.

The crystal structure reveals that the benzimidazole moiety is oriented largely parallel to the protein surface (Figure 5). Importantly, the carbon atom at position 4 (green circle) is directly positioned above the hydrophobic pocket providing ideal position for an exit vector into the transient pocket. The benzimidazole moiety therefore represents a promising scaffold for future optimization, analogous to inhibitor **2**.

Owing to the moderate resolution of 2.92 Å, some atoms remain undefined in the density (see Supporting Information) when compared to the other better resolved structures (Table 1). This also involves the C-terminal indole ring of the first molecule in the asymmetric unit that is not fully defined in the difference electron density map.

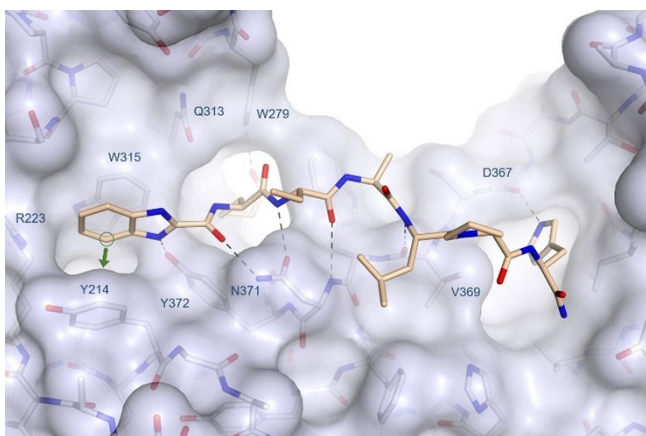


Figure 5. Interaction pattern of **3** (yellow, PDB ID: 5MHO) with FXIIIa^o. The benzimidazole is located perpendicular to the protein surface and may be used as a scaffold for occupying the hydrophobic pocket (green arrow).

Due to the commercial availability of derivatives, the methyl thiazole was used as preferred scaffold to address the hydrophobic pocket. Accordingly, we attached an ethyl ester at the methyl group of **2** and it turned out to be an excellent functional group at this exit vector.

Inhibitor **4** (ZED2360) bearing the ethyl ester at the thiazole was crystallized in complex with FXIIIa^o. The collected dataset showed a moderate resolution of 2.48 Å. Nevertheless, the inhibitor is decisively defined by the difference electron density (see the Supporting Information).

As anticipated, the crystal structure shows that the ethyl group of the ester introduced at the thiazole moiety is deeply buried in the hydrophobic pocket in the α -space (Figure 6). Moreover, the ester carbonyl oxygen serves as an H-bond acceptor for the guanidinium NH of Arg223, and the other ester oxygen accepts a hydrogen bond of the phenolic hydroxyl group of Tyr372. The remaining hydrogen bonds to the peptidic backbone are similarly established as already found for **2** and **3**.

Considering the geometry and the interaction pattern, the thiazole ester fits perfectly well into the complementary binding pocket of FXIIIa^o within the α -space. This is also reflected by a significantly improved binding affinity. The IC_{50} of **4** amounts 29 nM and exceeds that of **1** by almost a half order of magnitude. However, it must be considered that the inhibitors do not only differ within the α -space but **4** exhibits a terminal proline. Nevertheless, as a comparison of **1** with **2** and **3** the C-terminal proline takes only minor influence on the affinity. Thus, we explain major portion of the affinity enhancement of **4** to the modification in the α -space.

The conformational flexibility of Arg223 next to the active site might help to explain the yet unclear substrate specificity of FXIII.^[25–27] The identified flexible side chain can be of importance to either accommodate hydrophobic residues or acidic side chains. The flexibility of the α -space, along with the adaptive character of the β -space also involving a transient opening of a hydrophobic pocket as indicated in our previous contribution in 2013,^[24] suggest why a unique consensus

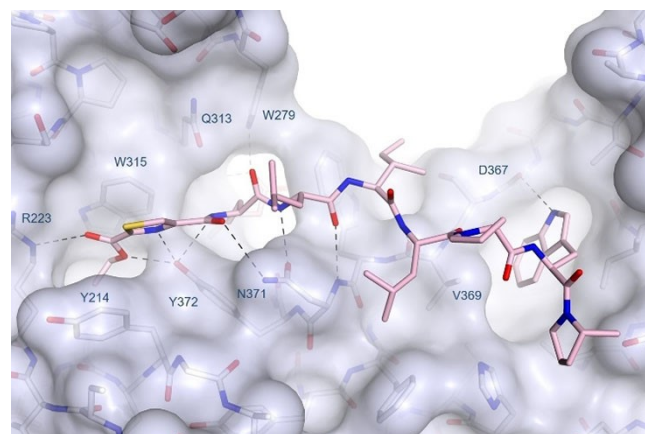


Figure 6. Interaction pattern of ZED2360 (pink, PDB ID: 5MHN) with FXIIIa^o. The ethyl group of the thiazole ester occupies the hydrophobic pocket. The ester oxygen atoms are positioned by H-bonds to Arg223 and Tyr372; the hydrophobic pocket is lined by Tyr214 and Trp315.

sequence of FXIII substrates seems to be lacking. Obviously, FXIII is a perfect example to study the properties of transient binding pockets.

Remarkably, residues forming the novel hydrophobic pocket in the α -space are highly conserved (Figures S1 and S2 in the Supporting Information) within the human transglutaminase family. Only positions 214 (FXIII: Tyr) and 223 (FXIII: Arg) differ in their side chain more distinctly. However, both amino acids possess hydrophobic character next to the α -carbon atom. In the crystal structure of TG2 and TG3 the hydrophobic pocket is not formed (Figure S1). But on closer consideration, in both structures the hydrophobic pocket can be opened by conformational adaptation of the respective side chains (TG2: Gln169, TG3: Val164, Ile173, Arg247). Conclusively, addressing the hydrophobic pocket in the α -space can be a proper approach for the development of inhibitors for human transglutaminases in general.

Conclusion

Occupation of the hydrophobic pocket in the α -space by well-selected ligand portions proved to be a promising strategy to improve binding affinity of the initial lead compound **1**. Substitution of the N-terminal acetylated aspartate of **1** by a methyl thiazole group (**2**) provides a starting point for occupying the hydrophobic pocket of the α -space. Additionally, adding an ethyl ester substituent (**4**) of which the ethyl substituent fills the hydrophobic pocket improves binding into low two-digit nanomolar range.

The shallow surface-exposed active site renders FXIII and similarly other transglutaminases to challenging targets for drug design. Thus, recovering the transient hydrophobic pocket in the α -space and its occupation represents an important step in direction of the ultimate goal of finding reversible low-molecular-weight FXIII inhibitors for oral administration of antithrombotic therapy.

Experimental Section

Expression and purification

The functional expression of recombinant FXIII-A₂ (A subunits) in insect cells, its respective purification and the synthesis of Michael acceptor (MA) transglutaminase blockers was recently described^[28] and will be briefly summarized below. Activation of blood coagulation factor XIII was achieved by high calcium ion concentrations instead of exposure to thrombin.^[29] A solution of purified recombinant FXIII-A₂ (0.2 mg/mL) in 10 mM Tris-HCl, pH 8.0, 300 mM NaCl, 15% (v/v) glycerol containing 100 mM Ca²⁺ was mixed with the inhibitor at a molar ratio of 1:25. The mixture was stirred and incubated at room temperature for 1 h. The inhibited complex was concentrated and subsequently applied to a Superdex75 pg HiLoad gel filtration column equilibrated with 10 mM Tris-HCl pH 8.0, 300 mM NaCl, 15% (v/v) glycerol containing 3 mM CaCl₂.

Synthesis

The inhibitors ZED1630, ZED2360 and ZED2369 are modified peptides derived from phage display screening^[27] containing a Michael Acceptor as substrate glutamine mimetic. The syntheses were performed by standard Fmoc solid-phase peptide chemistry^[30] (reactions in DMF, coupling with TBTU/HOBt/DIPEA, deprotection with piperidine) using Fmoc Rink Amide MBHA resin as starting material yielding the respective peptides as free amines (unprotected N terminus) after cleavage from the resin (with TFA/water/triisopropylsilane 95:2.5:2.5). The final inhibitors were synthesized by coupling of the respective carboxylic acid (in DMF, using HATU/DIPEA). Purification was performed by reverse phase HPLC. Identity was confirmed by mass spectrometry, purity was >95%, as analyzed by HPLC at 214 nm. The synthesis of ZED1301 was described elsewhere.^[24]

A more detailed description of the inhibitor synthesis can be found in a patent from 2016.^[31]

Isopeptidase assay

The binding affinity of the inhibitors was measured by an isopeptidase assay.^[32] Factor XIIIa cleaves a dark quenching molecule from the side chain of a modified dodecapeptide based on the N-terminal sequence of α_2 -antiplasmin. Subsequently, the fluorescence of an N-terminal coupled dye increases and can be monitored on-line ($\lambda_{\text{ex}}=313$ nm; $\lambda_{\text{em}}=418$ nm).

12 μ L recombinant human FXIII-A₂ (25 μ g/mL, T027, Zedira) or FXIII-A₂B₂ derived from human plasma (T007) (50 μ g/mL) and 3 μ L human α -thrombin (0.5 U/mL, T056, Zedira) were mixed with 270 μ L assay buffer (50 mM Tris-HCl, 10 mM CaCl₂, 150 mM NaCl, 5.56 mM glycine methyl ester, 5 mM DTT, pH 7.5) containing 55 μ M A101 substrate. The mixture was incubated for 20 min at room temperature to activate FXIII. 15 μ L of inhibitor solution (serial dilution from 1.25 μ M to 1.25 nM) dissolved in DMSO/assay buffer were added, mixed and the kinetic measurement started after 3 min. Fluorescence emission was monitored 37 °C for 30 min using a CLARIOstar fluorescence micro plate reader (BMG Labtech, Ortenberg, Germany). The respective IC₅₀ values were calculated by non-linear regression using the MARS software package (BMG Labtech).

The increase in fluorescence (DRFU) is measured using $\lambda_{\text{ex}}=313$ nm and $\lambda_{\text{em}}=418$ nm at 37 °C for 30 min in serial dilution. For each concentration, the FXIII activity (DRFU, "slope") is determined between 20 and 30 min (linear range). The residual enzyme activity (%) is determined by dividing the respective DRFU by the DRFU of the control (enzyme activity without inhibitor). Plotting the residual enzyme activity (%) over the enzyme concentrations results in the "IC₅₀"-curve by "4-parameter-fit". To simplify, IC₅₀ values were determined as inhibitor concentrations at which 50% of the initial FXIII activity is blocked.

Crystallization, data collection and structure determination

The eluted protein was concentrated to 10 mg/mL and protein crystals were grown at ambient temperature using the hanging drop vapor diffusion method. Crystallization was achieved by mixing 5 μ L protein solutions with 5 μ L precipitation solution (170 mM ammonium sulphate, 85 mM sodium cacodylate pH 6.5, 25.5% (w/v) PEG 8,000, 15% (v/v) glycerol). Crystals of FXIIIa^o in complex with the inhibitors were flash-frozen in liquid nitrogen and datasets were collected at the BESSY II electron storage ring.^[33] All data sets were processed in space group P1 by using the programs HKL2000^[34] (ZED1630) and XDS^[35] (ZED2360, ZED2369). The initial

phases were calculated by Fourier synthesis using the structure (PDB ID: 4KTY) as starting model in the first refinement step with Phenix.^[36] The model was manually improved with Coot^[37] and refined with Phenix. In the beginning, the structure was refined as rigid body, whereas both molecules of the asymmetric unit were split into the four domains. Subsequently, simulated annealing was performed. All structures were refined with coordinates, occupancies and individual B-factors (group B-factor for ZED2369 because of the low resolution). Restraints of the ligands were generated by GRADE.^[38]

Abbreviations

DIPEA	<i>N,N</i> -diisopropylethylamine
DMF	dimethylformamide
Fmoc	fluorenylmethoxycarbonyl; HATU: 2-(7-aza-1 <i>H</i> -benzo- triazole-1-yl)-1,1,3,3-tetramethyluronium hexafluoro- phosphate
HOBt	hydroxybenzotriazole
MBHA	methylbenzhydrylamine
TBTU	<i>O</i> -(benzotriazol-1-yl)- <i>N,N,N',N'</i> -tetramethyluronium tetra- fluoroborate
TFA	trifluoroacetic acid

Acknowledgements

We thank the beamline staff of BESSY II (Helmholtz-Zentrum Berlin) for data collection support and acknowledge the support by a travel grant from the Helmholtz-Zentrum Berlin. We also would like to thank Christiane Pelzer for IC_{50} measurements, Dr. Andreas Heil for proof reading the manuscript and Katrin Bott-Fischer for finalization of the figures. Financial support by the German Ministry of Education and Research (BMBF) is gratefully acknowledged (FKZ 0316030).

Conflict of Interest

The authors declare no conflict of interest.

Keywords: anticoagulants · crystal structure analysis · factor XIII · structure-activity relationship · transglutaminase

- [1] L. Lorand, R. M. Graham, *Nat. Rev. Mol. Cell Biol.* **2003**, *4*, 140.
- [2] D. Aeschlimann, V. Thomazy, *Connect. Tissue Res.* **2000**, *41*, 1.
- [3] S. Y. Kim, S. I. Chung, K. Yoneda, P. M. Steinert, *J. Invest. Dermatol.* **1995**, *104*, 211.
- [4] E. Candi, S. Oddi, A. Terrinoni, A. Paradisi, M. Ranalli, A. Finazzi-Agro, G. Melino, *J. Biol. Chem.* **2001**, *276*, 35014.
- [5] E. Candi, S. Oddi, A. Paradisi, A. Terrinoni, M. Ranalli, P. Teofoli, G. Citro, S. Scarpato, P. Puddu, G. Melino, *J. Invest. Dermatol.* **2002**, *119*, 670.
- [6] K. Laki, L. Lorand, *Science* **1948**, *108*, 280.
- [7] S. Gundemir, G. Colak, J. Tucholski, G. V. Johnson, *Biochim. Biophys. Acta* **2012**, *1823*, 406.

- [8] J. S. K. Chen, K. Mehta, *Int. J. Biochem. Cell Biol.* **1999**, *31*, 817.
- [9] S. Mishra, L. J. Murphy, *J. Biol. Chem.* **2004**, *279*, 23863.
- [10] S. Mishra, A. Saleh, P. S. Espino, J. R. Davie, L. J. Murphy, *J. Biol. Chem.* **2006**, *281*, 5532.
- [11] J. Wodzinska, *Mini-Rev. Med. Chem.* **2005**, *5*, 279.
- [12] L. Lorand, *J. Thromb. Haemostasis* **2005**, *3*, 1337.
- [13] L. Lorand, P. T. Velasco, S. N. P. Murthy, P. Lefebvre, D. Green, *Blood* **1999**, *93*, 909.
- [14] A. M. Sulic, K. Kurppa, T. Rauhavirta, K. Kaukinen, K. Lindfors, *Expert Opin. Ther. Targets* **2015**, *19*, 335.
- [15] R. Pasternack, C. Buchold, R. Jahnig, C. Pelzer, M. Sommer, A. Heil, P. Florian, G. Nowak, U. Gerlach, M. Hils, *J. Thromb. Haemostasis* **2019**, e14646.
- [16] W. Dieterich, T. Ehnis, M. Bauer, P. Donner, U. Volta, E. O. Riecken, D. Schuppan, *Nat. Med.* **1997**, *3*, 797.
- [17] L. Huang, J. L. Haylor, Z. Hau, R. A. Jones, M. E. Vickers, B. Wagner, M. Griffin, R. E. Saint, I. G. Coutts, A. M. El Nahas, T. S. Johnson, *Kidney Int.* **2009**, *76*, 383.
- [18] R. L. Eckert, M. T. Kaartinen, M. Nurminskaya, A. M. Belkin, G. Colak, G. V. Johnson, K. Mehta, *Physiol. Rev.* **2014**, *94*, 383.
- [19] C. Tabolacci, A. De Martino, C. Mischiati, G. Feriotto, S. Beninati, *Med Sci (Basel)* **2019**, *7*, 19.
- [20] I. Komaromi, Z. Bagoly, L. Muszbek, *J. Thromb. Haemostasis* **2011**, *9*, 9.
- [21] L. Muszbek, Z. Bereczky, Z. Bagoly, I. Komaromi, E. Katona, *Physiol. Rev.* **2011**, *91*, 931.
- [22] L. Muszbek, Z. Bagoly, Z. Bereczky, E. Katona, *Cardiovasc. Hematol. Agents Med. Chem.* **2008**, *6*, 190.
- [23] V. C. Yee, L. C. Pedersen, I. Letrong, P. D. Bishop, R. E. Stenkamp, D. C. Teller, *Proc. Natl. Acad. Sci. USA* **1994**, *91*, 7296.
- [24] M. Stieler, J. Weber, M. Hils, P. Kolb, A. Heine, C. Buchold, R. Pasternack, G. Klebe, *Angew. Chem. Int. Ed.* **2013**, *52*, 11930.
- [25] P. G. Doiphode, M. V. Malovichko, K. N. Mouapi, M. C. Maurer, *Anal. Biochem.* **2014**, *457*, 74.
- [26] C. L. Nikolajsen, T. F. Dyrland, E. T. Poulsen, J. J. Enghild, C. Scavenius, *J. Biol. Chem.* **2014**, *289*, 6526.
- [27] Y. Sugimura, M. Hosono, F. Wada, T. Yoshimura, M. Maki, K. Hitomi, *J. Biol. Chem.* **2006**, *281*, 17699.
- [28] A. Heil, J. Weber, C. Buchold, R. Pasternack, M. Hils, *Thromb. Res.* **2013**, *131*, e214.
- [29] R. B. Credo, C. G. Curtis, L. Lorand, *Proc. Natl. Acad. Sci. USA* **1978**, *75*, 4234.
- [30] W. C. Chan, P. D. White, *Fmoc solid phase peptide synthesis, A practical approach*, Oxford University Press, **2000**, p. 41.
- [31] C. Buchold, U. Gerlach, M. Hils, R. Pasternack, J. Weber (ZEDIRA GMBH, Darmstadt (Germany)), US 9,434,763 B2, Sept. 6, **2016**.
- [32] K. Oertel, A. Hunfeld, E. Specker, C. Reiff, R. Seitz, R. Pasternack, J. Dodt, *Anal. Biochem.* **2007**, *367*, 152.
- [33] U. Mueller, N. Darowski, M. R. Fuchs, R. Forster, M. Hellmig, K. S. Paithankar, S. Puhlinger, M. Steffien, G. Zocher, M. S. Weiss, *J. Synchrotron Radiat.* **2012**, *19*, 442.
- [34] Z. Otwinowski, W. Minor, *Methods Enzymol.* **1997**, *276*, 307.
- [35] W. Kabsch, *Acta Crystallogr. Sect. D* **2010**, *66*, 125.
- [36] P. D. Adams, P. V. Afonine, G. Bunkoczi, V. B. Chen, I. W. Davis, N. Echols, J. J. Headd, L. W. Hung, G. J. Kapral, R. W. Grosse-Kunstleve, A. J. McCoy, N. W. Moriarty, R. Oeffner, R. J. Read, D. C. Richardson, J. S. Richardson, T. C. Terwilliger, P. H. Zwart, *Acta Crystallogr. Sect. D* **2010**, *66*, 213.
- [37] P. Emsley, B. Lohkamp, W. G. Scott, K. Cowtan, *Acta Crystallogr. Sect. D* **2010**, *66*, 486.
- [38] O. S. Smart, T. O. Womack, A. Sharff, C. Flensburg, P. Keller, W. Paciorek, C. Vonrhein, G. Bricogne, GRADE web server, Cambridge, United Kingdom, Global Phasing Ltd., <http://www.globalphasing.com>, **2012**.

Manuscript received: January 30, 2020
 Revised manuscript received: March 16, 2020
 Accepted manuscript online: March 17, 2020
 Version of record online: April 7, 2020